JOURNAL OF MATERIALS SCIENCE 21 (1986) 2628–2632

Fracture strength characterization of tubular ceramic materials using a simple c-ring geometry

M. K. FERBER
Department of Ceramic Engineering, University of Illinois at Urbana-Champaign, Urbana, Illinois 61801, USA

V. J. TENNERY, S. B. WATERS, J. OGLE
Metals and Ceramics Division, Oak Ridge National Laboratory, Oak Ridge, Tennessee 37831, USA

The potential application of the c-ring compression specimen for strength determinations involving tubular ceramic samples was investigated. Mathematical descriptions of the stress distributions generated within the c-ring were derived using several approaches. The resulting equations were used in conjunction with a Weibull analysis to predict a relationship between failure probability and fracture strength. Finally, the validity of the c-ring test was examined for a SiC ceramic by comparing the c-ring strength data with that obtained from four-point bend samples.

1. Introduction

Structural ceramics such as SiC, Si_3N_4 and Al_2O_3 have shown considerable potential for use in high-temperature heat recovery applications. Specific examples range from more traditional heat recuperators to heat exchangers (hx) employed in advanced fossil-energy conversion systems [1–4]. As indicated in Table I, hx elements, which often have a tubular geometry, can be subjected to significant levels of thermal and mechanical stress. Consequently, the high-temperature strength of the structural ceramic material can constitute a critical factor in hx design.

In the case of tubular hx materials, techniques for making reliable strength measurements are somewhat limited. The use of more conventional bend-bar samples for tubular elements requires complicated machining techniques which generally alter the intrinsic surface-flaw population. In studies aimed at examining the influence of environment upon the strength, such machining could significantly limit the environmental sensitivity of the resulting measurements. An attractive alternative for strength determinations in tubular samples involves the use of a c-ring diametral test [5, 6] (Fig. 1). Because of the simple geometry, the specimens can be easily fabricated with minimal machining. In addition, the compressive loading facilitates measurements at elevated temperatures. Since the maximum tensile stress is generated along the outer diameter, the test is quite sensitive to surface flaws as well as to changes in the flaw population induced by environmental factors.

Because of the apparent utility of the c-ring diametral test for strength studies involving tubular samples, this paper considers the technique in some detail. First, mathematical descriptions of the stress distributions generated in the c-ring are derived. This information is then used in conjunction with a Weibull analysis to predict the relationship between failure probability and fracture strength. Finally, the validity of the test is examined for a silicon carbide ceramic by comparing the c-ring strength data with those obtained from four-point bend tests.

2. Mathematical treatment

2.1. Stress distributions

The c-ring stress distributions can be determined using several approaches. For example, the tangential stress σ_θ in the c-ring can be estimated from simple bending theory for curved beams [5]. In this method, one considers the equilibrium requirements associated with a typical section of the c-ring located at an angle θ from the midplane (Fig. 1b). To maintain equilibrium, a vertical force P and bending moment M, where $M = P(r_o + r_i)\cos\theta/2$, must be applied at this section. Using formulae for the bending of curved beams [5] one can show that

$$\sigma_\theta = \frac{P}{A}\frac{R(r - r_a)}{r(R - r_a)}\cos\theta \quad (1a)$$

where

$$r_a = (r_o + r_i)/2 \quad (1b)$$

$$R = \frac{(r_o - r_i)}{\ln(r_o/r_i)} \quad (1c)$$

and

$$A = (r_o - r_i)w \quad (1d)$$

In these equations P is the break load (negative for compressive loading), R is the moment of inertia, and w is the c-ring thickness. The term (P/A) in Equation 1a represents a constant compressive stress arising from the uniform vertical loading ($= P\cos\theta$), while the second term is due to the bending moment.

0022–2461/86 $03.00 + .12

TABLE I Potential sources of stress in heat-exchanger applications

Thermal stresses can arise from:
1. Temperature gradients established in response to steady-state heat flow.
2. Rapid unexpected fluctuations in temperature (transient behaviour).
3. Mismatch in thermal expansion.

Mechanical stresses are generated from:
1. Bending moments arising from gravity loading (important only in the case of long horizontal tubes).
2. External loads required for maintenance of joints and tube/header seals.
3. Internal pressurization of hx elements involved in operation of hot gas turbine.

A second approach for determining the c-ring stress distributions involves the application of a formal elastic analysis. As an initial simplification, the c-ring loading configuration is approximated by a curved bar with one end constrained and the other subjected to a shear force P (Fig. 2). The corresponding elastic treatment [7] yields the following expressions for the tangential, radial and shear stresses (σ_θ, σ_r and $\tau_{r\theta}$, respectively):

$$\sigma_\theta = (P/A)F(r)\cos\theta \quad (2a)$$

$$\sigma_r = (P/A)G(r)\cos\theta \quad (2b)$$

and

$$\tau_{r\theta} = -(P/A)G(r)\sin\theta \quad (2c)$$

The functions $F(r)$ and $G(r)$ are given as

$$F(r) = \frac{1}{N}\left[\frac{r_o^2 + r_i^2}{r} + \frac{(r_o r_i)^2}{r^3} - 3r\right] \quad (3a)$$

and

$$G(r) = \frac{1}{N}\left[\frac{r_o^2 + r_i^2}{r} - \frac{(r_o r_i)^2}{r^3} - r\right] \quad (3b)$$

where

$$N = r_i^2 - r_o^2 + (r_o^2 + r_i^2)\ln\frac{(r_o/r_i)}{r_o - r_i} \quad (3c)$$

Since the configuration in Fig. 2 approximates a compressively loaded c-ring, the P in Equations 2a to c is negative.

Fig. 3 illustrates the radial dependence of σ_θ and σ_r based on Equations 2a and b. The dimensions of r_o, r_i

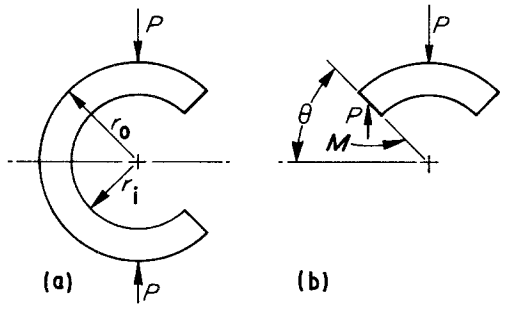

Figure 1 Schematic representative of c-ring diametral compression specimen illustrating (a) simple loading configuration and (b) loading requirements to maintain equilibrium at an arbitrary section.

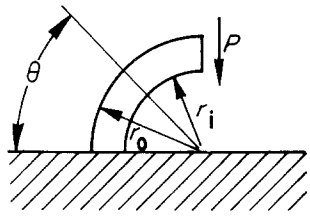

Figure 2 Loading configuration used to approximate c-ring specimen.

and w chosen for this calculation are characteristic of samples tested in this study. The stress distributions in this figure are associated with the c-ring midplane ($\theta = 0°$ in Fig. 1) in which case the shear stress ($\tau_{r\theta} = -\sigma_r \sin\theta/\cos\theta$) vanishes. As expected, the tangential stresses at $r = r_o$ are tensile while those at $r = r_i$ are compressive. Finally, the data in Fig. 3 reveal excellent agreement between the σ_θ distribution determined from the elastic treatment (Equation 3a) and that obtained from the simple bending expression (Equation 2a).

2.2. Failure probability

The probability of failure P_f for the c-ring specimen subjected to a stress distribution σ can be estimated from the two-parameter Weibull equation [8]

$$P_f = 1 - \exp\left[-\int_v (\sigma/\sigma_0)^m \, dV\right] \quad (4)$$

where m is the Weibull modulus and σ_0 is a scaling parameter. Equation 4 is valid only for the case of volume flaws. When surface flaws control the strength, the integral is evaluated over the surface area.

Since the tangential stresses are significantly larger than either the radial or shear stresses (particularly in the region where failure occurs, radial or shear stresses (particularly in the region where failure occurs, $\theta \approx 0°$), then the σ in Equation 4 can be replaced by σ_θ. Using Equation 1a for σ_θ, the Weibull expression becomes

$$\ln[(1 - P_f)^{-1}] = \left(\frac{\sigma_\theta^{max}}{\sigma_0}\right)^m \int_v \left(\frac{\sigma_\theta}{\sigma_\theta^{max}}\right)^m r\,dr\,d\theta\,dz \quad (5a)$$

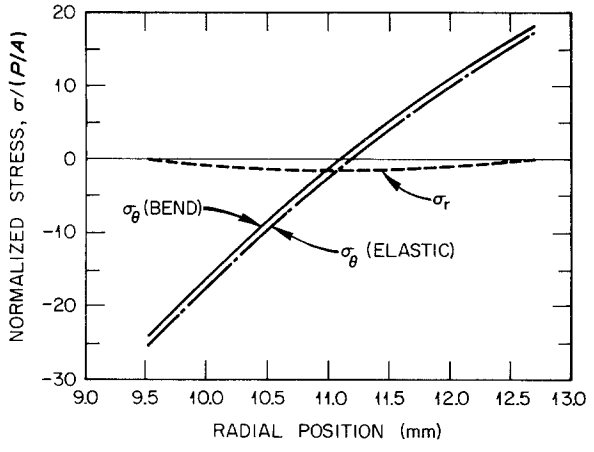

Figure 3 Radial dependence of σ_θ and σ_r stresses determined from elastic treatment of c-ring. The σ_θ radial distribution based on the simple bending equations is shown for comparison. r_o = 12.7 mm, r_i = 9.5 mm, w = 6.4 mm, θ = 0°.

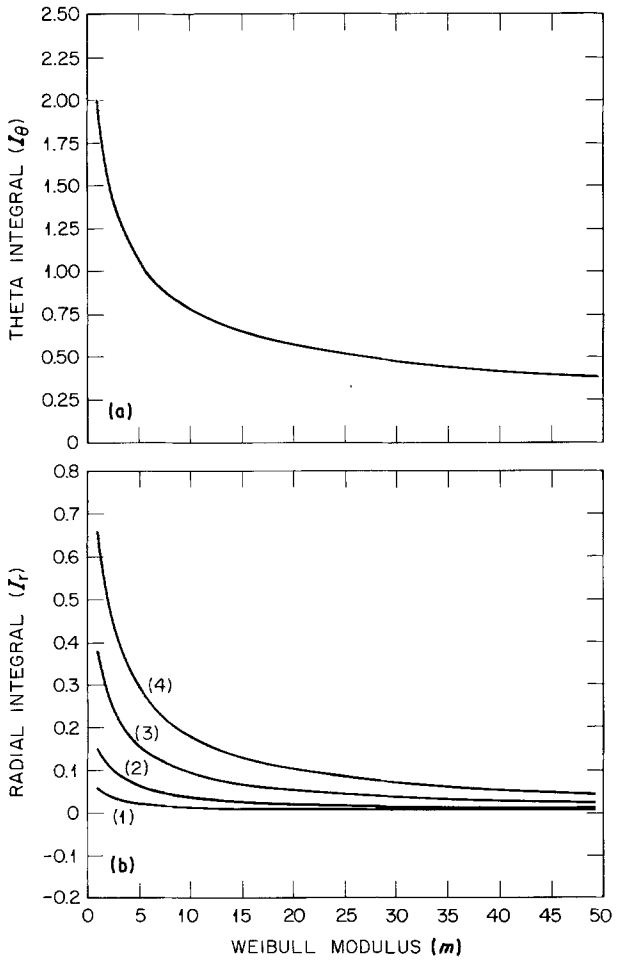

Figure 4 Results of numerical integration. Values of r_o/r_a as follows: (1) 1.10, (2) 1.25, (3) 1.50, (4) 1.75.

where σ_θ^{max} is the maximum tensile stress ($\theta = 0°$ and $r = r_o$) and

$$\frac{\sigma_\theta}{\sigma_\theta^{max}} = \frac{(r - r_a)r_o}{(r_o - r_a)r}\cos\theta \quad (5b)$$

By defining the integrals I_θ and I_r as

$$I_\theta = 2\int_0^{\pi/2} \cos^m\theta \, d\theta \quad (6a)$$

and

$$I_r = \int_1^{r_o/r_a} \left(\frac{1 - 1/x}{1 - r_a/r_o}\right)^m x \, dx \quad (6b)$$

one can show that

$$\ln [(1 - P_f)^{-1}] = \left(\frac{\sigma_\theta^{max}}{\sigma_0}\right)^m w r_a^2 I_r I_\theta \quad (6c)$$

When surface flaws control the strength, Equation 6c becomes

$$\ln [1 - P_f)^{-1}] = \left(\frac{\sigma_\theta^{max}}{\sigma_0}\right)^m (2r_a^2 I_\theta I_r + w r_o I_\theta) \quad (7)$$

Values of I_θ and I_r (determined using numerical integration) are given as a function of m in Figs 4a and b, respectively. Notice that I_r also depends upon the r_o/r_a ratio in accordance with Equation 6b.

3. Experimental procedure

To examine the validity of the c-ring technique, tubular specimens of a commercially-available sintered, alpha silicon carbide (α-SiC)* were sectioned into c-ring and bend-bar samples as shown in Fig. 5. The tensile surfaces of all samples were ground with a 70 μm diamond wheel with the grinding direction parallel to either the long dimension of the prismatic bar or the circumference of the c-ring. The tensile edges were also bevelled with a 30 μm diamond wheel. The average dimensions of each specimen type are given in Table II.

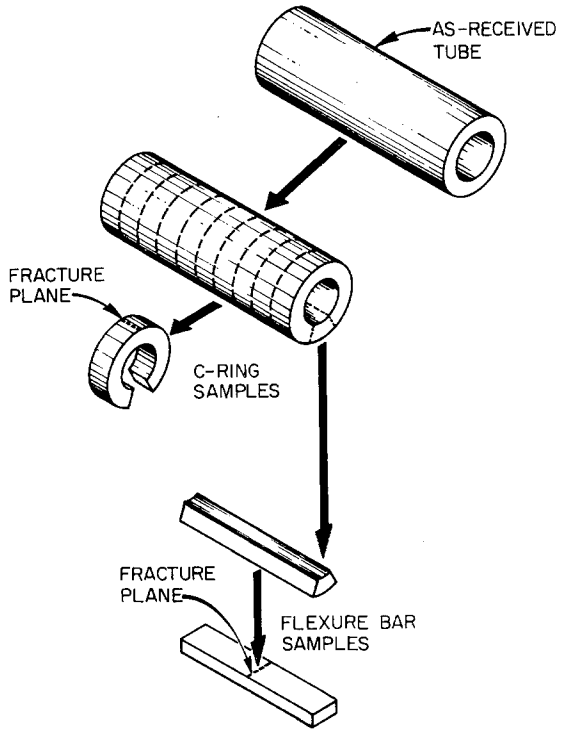

Figure 5 Sectioning procedure used to fabricate c-ring and bend bar samples from α-SiC tubular elements.

The samples were fractured at room temperature in an Instron machine (Instron Corp., Canton, Massachusetts) operating at a cross-head speed of 8.5 μm sec^{-1} (0.02 in. min^{-1}). The rectangular bars were tested in four-point bending using an inner and outer span of 6.35 mm (0.25 in.) and 19.05 mm (0.75 in.) respectively. The resulting data were fitted to the two-parameter Weiball equation [8]

$$\ln \ln [(1 - P_f)^{-1}] = m \ln (\sigma_b^{max}/\sigma_0) + \ln K \quad (8a)$$

where

$$\sigma_b^{max} = 0.75 P_f/bh^2 \quad (8b)$$

$$K = VK_v = \frac{0.33m + 1}{2(m + 1)^2} \quad (8c)$$

TABLE II Average dimensions of c-ring and bend-bar specimens

C-ring	Bend-bar*
r_o = 12.5 mm	b = 3.1 mm
r_i = 9.3 mm	h = 2.6 mm
w = 5.2 mm	L = 20.3 mm
r_o/r_a = 1.15 mm	

*b is the width, h the height and L the length of the bend-bar specimen.

*Iso-pressed Hexaloy SA SiC, Carborundum Co., Niagara Falls, New York.

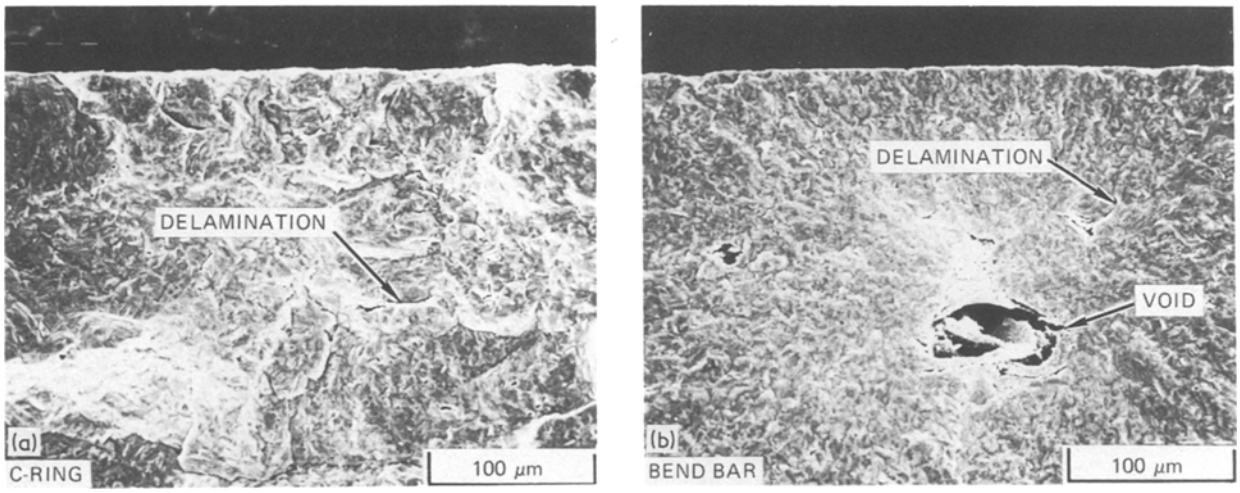

Figure 6 SEM examination of fracture surfaces. Subsurface volume flaws generally acted as failure sites in both (a) c-ring and (b) four-point bend samples.

for volume flaws, and

$$K = AK_a = AK_v(0.54m + 1) \quad (8d)$$

for surface flaws [8]. In these equations, σ_b^{max} is the maximum tensile stress at the fracture load P_f, V is the volume of the bend bar and A is its surface area. A linear regression analysis was used to estimate m and σ_0 for both volume and surface flaws.

The c-ring samples were compressively loaded to failure. The m and σ_0 parameters were determined for surface- and volume-controlled fracture by fitting the experimental P_f and σ_θ^{max} quantitites to Equations 5b, 6a to c and 7. The values of I_θ and I_r required for the analysis were obtained by numerically integrating Equations 6a and b, respectively.

The failure probability P_f was estimated from the expression [8]

$$P_f = (n - 0.5)/N_t \quad (9)$$

where N_t is the total number of samples tested and n is the rank of a particular specimen. The ranking is from the lowest ($n = 1$) to highest ($n = N$) fracture stress σ^{max}.

4. Results and discussion

The average fracture strengths (σ^{max}) and standard deviations for the c-ring and bend-bar samples were 237 ± 36.MPa (34.4 ± 5.1 ksi) and 336 ± 51 MPa (48.7 ± 7.4 ksi), respectively. These results were compiled from tests involving 19 c-ring and 31 bend-bar specimens. As discussed below, the lower c-ring strength could not be entirely attributed to a statistical volume effect.

Subsequent examinations of the fracture surfaces of several samples with an SEM indicated that failure was controlled primarily by volume flaws. As shown in Fig. 6, these flaws were present as either sperical voids or narrow delaminations, each having a maximum dimension of 50 to 80 μm.

The c-ring and bend-bar Weibull distributions are shown in Fig. 7. The values of σ_0 given for this figure were calculated on the basis of volume-controlled failure in accordance with the SEM observations. Since the distributions of flaws were identical in the two specimen types, one would expect the corresponding m and σ_0 quantities to be similar. While this was true for the Weibull moduli, the corresponding values of σ_0 were in considerable disagreement. This discrepancy implies that the statistical volume effect could not adequately account for the lower c-ring strengths. To further illustrate this point, the c-ring strength distribution was predicted from the Weibull parameters obtained for the bend bars. As shown in Fig. 7, the c-ring strengths associated with the predicted distribution (dotted line) were significantly higher than the experimental values (at a given failure probability).

The only apparent difference between the c-ring and bend-bar failure characteristics concerned the orientation of the fracture plane with respect to the original tube. As illustrated in Fig. 5, the c-ring failure plane was perpendicular to that of the bend specimen. Consequently, the discrepancy in the σ_0 values may have been related to an anisotropic mechanical behaviour associated with the as-received α-SiC tubes.

To check for this possibility, the fracture toughness K_c on these two planes was measured using the indent-crack length method [9]. Specifically, K_c was determined from the crack lengths propagated from a diamond pyramid indentation according to the equation

$$\frac{K_c}{H(r^{1/2})}\left(\frac{H}{E}\right)^{2/5} = F\left(\frac{c}{r}\right) \quad (10)$$

where H is the hardness, E the Young's modulus, r the half-indent diagonal, c the crack length and $F(c/r)$ a polynomial function [9].

The resulting toughness associated with the bend-bar fracture plane was found to be 1.4 times larger than K_c for the c-ring failure plane. Therefore, the lower c-ring strengths at a given P_f were due not only to a volume effect but also to a reduced fracture resistance. To account for the anisotropic toughness behaviour in the Weibull analysis, the maximum c-ring strength values σ_θ^{max} were normalized with respect to the bend-bar K_c by multiplying σ_θ^{max} by 1.4. A subsequent regression analysis of the c-ring data then gave a σ_0 of 141 MPa.

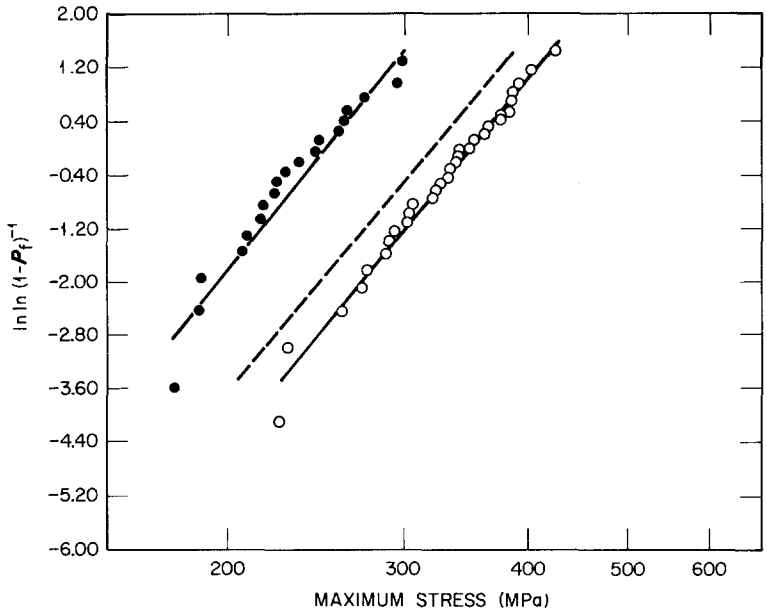

Figure 7 Comparison of c-ring and bend-bar strength distributions for α-SiC. (●) c-ring with m = 8.04, σ_0 = 101 MPa; (○) flexure bar with m = 7.87, σ_0 = 122 MPa; (– – –) predicted c-ring distribution.

The fact that the corrected σ_0 is signifcantly larger than the value calculated from the bend-bar distribution suggests that additional factors were responsible for the experimental variations in the two strength distributions. One possibility is that the geometries of the volume flaws were slightly different for the two fracture-plane orientations. These geometry effects would not be detected in the indent toughness testing since well-defined, semi-circular flaws were involved. Theoretically, the statistical analysis could be modified to account for the effects of crack geometry [10, 11]. Unfortunately, the lack of specific information concerning this geometry (for both types of volume flaw present) precludes this more rigorous treatment.

5. Conclusions

Expressions describing the stress distributions generated in a compressively loaded c-ring specimen were developed using simple bending theory and a more formal elasticity approach. The dominant stress was the tangential component σ_θ which was tensile at the outer surface and compressive at the inner surface. The distributions of σ_θ given by the two mathematical treatments were found to be in excellent agreement.

The σ_θ stress distribution was then used in conjunction with a two parameter Weibull analysis to predict the c-ring failure probability P_f. Due to the complex nature of the equation describing σ_θ, numerical integration was required for this analysis.

A comparison of the strength distributions obtained for c-ring and bend-bar specimens prepared from an α-SiC tube revealed good agreement between the corresponding Weibull moduli. However, at a given P_f, the reduction in the c-ring strength could not be adequately explained on the basis of a statistical volume effect. These large strength differences, which were also reflected by a significant discrepancy in the respective σ_0 values, could in part be attributed to anisotropy in the fracture toughness associated with the as-received α-SiC tube.

References

1. V. K. NANGIA, "Materials for Coal Conversion and Use", Vol. II, Parts 1 and 2, DOE Report FE-2468-59 (Engineering Societies Commission on Energy, Washington DC, 1979) p. 9–18.
2. D. J. McFARLIN, C. T. SGAMBOTI and R. D. LESSARD, "Ceramic Heat Exchanger Applications Study", UTRC82-34 (United Technologies Research Center, East Hartford, Connecticut, 1982) p. 1–13.
3. M. COMBS, D. KOTCHICK and H. WARREN, "High-Temperature Ceramic Heat Exchanger", EPRI FP-1127 (Airesearch Manufacturing Company of California, Torrence, California, 1979) p. 1.1–2.21.
4. V. J. TENNERY, "Economic Application, Design Analyses, and Material Availability for Ceramic Heat Exchangers", ORNL/TM-7680 (Oak Ridge National Laboratory, Oak Ridge, Tennessee, 1981) p. 1–65.
5. J. N. CERNICA, "Strength of Materials" (Holt, Reinehart and Winston, New York, 1966) p. 205.
6. J. R. G. EVANS and R. STEVENS, *J. Br. Ceram. Trans.* **83** (1984) 14.
7. S. P. TIMOSHENKO and J. N. GOODINER, "Theory of Elasticity" (McGraw-Hill, New York, 1970) p. 443.
8. C. A. JOHNSON, "Fracture Statistics in Design and Application" Report 79-CRD 212 (General Electric Co., Schenectady, New York, 1979).
9. A. G. EVANS, "Fracture Mechanics Applied to Brittle Materials", edited by S. W. Freiman, (Special Technical Publication No. 678, ASTM, Philadelphia, 1979) p. 112.
10. S. B. BATDORF and J. G. CROSE, *J. Appl. Mech.* **41**(2) (1974) 459.
11. S. B. BATDORF and H. L. HEINISCH, Jr, *J. Amer. Ceram. Soc.* **61**(7/8) (1978) 355.

Received 15 July
and accepted 12 August 1985